Ewa Cukrowska, Ignacy Cukrowski and Josef Havel, *S. Afr. J. Chem.*, 2000, **53** (3), 213-231, <http://journals.sabinet.co.za/sajchem/>, <http://ejour.sabinet.co.za/images/ejour/chem/chem_v53_n3_a5.pdf>.
[formerly: Ewa Cukrowska, Ignacy Cukrowski and Josef Havel, S. Afr. J. Chem., 2000, 53 (3), 5. (19pp.), <http://ejour.sabinet.co.za/images/ejour/chem/chem_v53_n3_a5.pdf>.]

Application of Artificial Neural Networks for Analysis of Highly Overlapped and Disturbed Differential Pulse Polarographic Peaks in the Region of Hydrogen Evolution

Ewa Cukrowska[‡], Ignacy Cukrowski[‡]* and Josef Havel[†]

[†] Department of Analytical Chemistry, Faculty of Science, Masaryk University, Kotlarska 2, 611 37 Brno, Czech Republic, e-mail: havel@chemi.muni.cz

[‡] Department of Chemistry, University of the Witwatersrand, Private Bag 3, WITS 2050, Johannesburg, South Africa; e-mail: ewa@aurum.chem.wits.ac.za; ignacy@aurum.chem.wits.ac.za

*) Corresponding author

Received on 12 October 2000, accepted on 10 November 2000

Abstract

Multivariate calibration based on a suitable experimental design (ED) and soft modelling with artificial neural networks (ANNs) is proposed for quantitative analysis of highly overlapped and disturbed differential pulse polarographic (DPP) peaks that occur in the region of a hydrogen evolution. It is demonstrated that analysis of mixtures, even if some of the constituents undergo an irreversible reduction and the background current varies significantly with a composition of a sample, can be quantified with reasonable accuracy using a combination of ED and ANNs. Examples of DPP examination of Zn^{II} and Cr^{III} mixtures and/or simultaneous determination of metal ions and a strong acid concentration are presented. The possibility of an on-line monitoring is suggested. It is demonstrated that standard hard model based refinement procedures perform much worse than ANNs combined with ED and, in principle, proved to be unsuitable for the purpose.

Keywords: artificial neural network, experimental design, differential pulse polarography, multicomponent analysis, zinc, chromium

1. Introduction

Electrochemical methods are used more often now with a growing need of chemical speciation of metal ions in environmental samples. One of the problems in resolving a mixture of several metal ions by electroanalytical techniques is often extensive overlap of the electrochemical signals.[1, 2] In many cases these might be in a form of broad and asymmetric responses. In addition, many environmental, industrial or biological samples are highly acidified.[3, 4] This creates a second problem, e.g. a peak resolution and determination of metal ions in the region of a hydrogen evolution.

The ANNs, the networks of artificial neurones, is a data processing system consisting of a large number of simple, highly interconnected processing elements in architecture inspired by the structure of the brain.[5-7] The applications based on ANNs used for data processing are called 'soft models', i.e. the models are able to represent the experimental behaviour of the system when the exact description is missing or is too complex. That is in contrast to so-called 'hard models', where the formulas and equations are known and the systems are exactly described by these equations and the values of physico-chemical constants.[8] The characteristics that make ANNs systems different from traditional computing are: (a) learning by example, (b) distributed associative memory, (c) fault tolerance and (d) pattern recognition.

Examples of applications of ANNs in analytical chemistry include non-linear calibration curves modelling[9-11] and quantitative analysis of multicomponent systems.[13-15] Good reviews on ANNs for chemists were written by Zupan and Gasteiger.[16–18] There are applications of ANNs in HPLC chromatography,[19-21] capillary electrophoresis,[22] electrokinetic micellar chromatography,[23] chiral separation,[24,25] and in ion chromatography,[26] for example. Anodic stripping voltammograms, in the form of well-shaped peaks of Zn^{II} and Cu^{II} were analysed by ANNs in the presence of intermetallic compounds formation.[27] A simultaneous determination of Pb^{II} and Cd^{II} in flow injection analysis with ANNs and DP voltammetric detection has also been demonstrated.[28] It has been shown that ANNs can be used in the case of highly overlapping, gaussian-type peaks obtained from differential pulse anodic stripping voltammetry[29] where negligible disturbance from the background current was observed, or in the potentiometric analysis of multicomponent solutions by nonselective sensors.[30]

In general, the ANNs processing can be performed using a conventional set of independent analysis. However, this could and possibly should be replaced by a statistically designed experimental protocol in which several factors are varied simultaneously. This multivariate approach reduces the number of experiments and improves statistical interpretation of results.[31, 32] The use of chemometric experimental design (ED) can be beneficial in the evaluation of electrochemical data. Also experimental variables such as temperature, ionic strength or acidity can be included in the analytical process. In this work the use of artificial neural networks and experimental design is examined for the analysis of differential pulse polarographic signals that are not suitable for any quantitative or qualitative analysis by 'conventional' means employing hard models. As an example, the simultaneous analysis of: (i) zinc^{II} and the acidity of a solution on which the DPP curve was recorded, and (ii) a mixture of chromium^{III} and zinc^{II}, when irreversible reduction process of chromium^{III} results in completely indistinguishable signal from the reduction of zinc^{II} in acidic medium, is described.

2. Experimental

2.1. Reagents

All reagents used were of analytical grade obtained from Merck. Triple distilled water used to prepare of solutions was from a quartz distillation system of Heraeus Quarzschmelze (Hanau, Germany). Stock solutions of Zn^{II} and Cr^{III} (0.01 M) were prepared by dilution from corresponding spectrophotometric standards. Acidity of samples was controlled by an addition of standardised nitric or perchloric acid. All experiments were performed at an ionic strength of 1 M in (H^+, K^+)NO_3 or (H^+, K^+)ClO_4 at 25ºC.

2.2. Apparatus and software

Differential pulse polarograms were obtained using the Autolab of EcoChemie (Utrecht, The Netherlands), the computerised electrochemical equipment joined with the electrochemical model 663 VA stand (Metrohm, Herisau, Switzerland). The system was operated and measurements performed using GPES2 software by EcoChemie. The multimode mercury electrode (Metrohm) was used as a working electrode in the mode of a static mercury drop. The reference and auxiliary electrode

were silver/silver chloride (3M KCl) and glassy carbon, respectively (both from Metrohm). High purity argon was used for oxygen removal and mixing of the solutions. Argon was passed over solutions when DP polarograms were recorded. Potential scan rate was 4 mV/s, pulse amplitude –50 mV and pulse duration 0.05 s. Drop time was set to 1 s. ANNs software used in this work was from the PDP package[6] processed on a Pentium-IBM-PC computer. The networks used were multilayered feedforward neural networks using as a learning scheme the algorithm of the back-propagation (BP) of errors and the generalised 'delta rule'[6] for the adjustment of the connection weights.

2.3. Procedure

All experimental solutions were prepared by dilution of metal stock solutions and standardised acids with respect to constant ionic strength (1 M). The purified argon was purged for 10 minutes through the samples, each of 5 ml in volume. DP polarograms were recorded in the potential range –0.8 to –1.15 and –0.6 to –1.2 V for the determination of Zn^{II} plus acidity of a sample, and Zn^{II} plus Cr^{III}, respectively. Measurements were repeated 2-3 times for each designed experiment.

The recorded DP polarograms have been stored in an ASCII format data files. They were used to create (i) the calibration matrix of learning sets, by applying a chosen pattern of experimental design, and (ii) the test sets. No electronic smoothing or filtering of acquired data was used. BP networks with three layers were created and optimisation of the artificial neural network parameters was then carried out varying systematically their values until the 'best' network performance was achieved in order to optimise the conditions for low errors of the prediction. Every second point was taken from polarograms to create the network's input layer. The hidden layer contained different number of neurones depending on the experiment's complexity. In the final structure of ANNs the lowest number of neurones in the hidden layer was used that generated acceptable results. The output layer was equal to the number of concentrations determined. The learning rate was usually kept low, from 0.001 to 0.005. To avoid an overtraining of ANNs, the training process was stopped when the change in the error was hundred times lower than calculated from the sum of squares of the differences between calculated and expected concentration values for the training set of solutions.

3. Results and Discussion

3.1. Simultaneous determination of Zn(II) and acidity of a sample

The calibration matrix for simultaneous determination of the zinc concentration and high acidity of a solution (from nitric acid) was constructed using an experimental design[31, 32] composed of two factors and three levels (Figure 1). Polarograms recorded for the training set are shown in Figure 2; the central 6/0.3 point seen in Figure 1 (e.g. 6×10^{-5} M Zn^{2+} in 0.3 M HNO_3) was recorded four times on separate samples as required by statistical validation of the ED employed. It is seen in Figure 2 that the DP polarograms are not suitable for a quantitative evaluation of the zinc content by 'traditional' means. Moreover, one would not be able to estimate the acidity of the samples studied at all. The results of ANNs evaluation for testing points are given in Table 1. The good agreement between the actual and computed by ANNs concentrations was satisfactory after training with ANNs structure containing only 3 neurones in the hidden layer. The higher number of neurones in the hidden layer has not changed results significantly, but allowed the training process with the same ED to be achieved in shorter time with a lower number of epochs. A good agreement between expected and computed values was obtained even for the lowest zinc concentration in the most acidic solution. Note that from polarograms recorded on solutions containing the lowest content of zinc one would not be able to predict the presence of this ion in a sample. It is obvious that it should also be possible to determine zinc simultaneously with other ions, such as copper, cadmium or lead (they are reduced at more positive potentials), in a number of samples where an acid/peroxide digestion would be required (electrochemical analysis of samples containing organic matter). It is seen in Figure 2 that to attempt any quantitative evaluation of the $zinc^{II}$ content by use of 'traditional' analytical approach the background current would have to be recorded first and subtracted from the polarogram recorded on a sample with $zinc^{II}$. This is not always possible when real samples are analysed. More importantly, however, the change in the background current in the absence and the presence of metal ions might take place, as is the case in this work. One can see in Figure 2 that the background current prior the reduction of zinc in unaffected by the zinc content, but at high and negative values of the applied potential the increase in the hydrogen evolution is observed with an increase in the zinc concentration. The use of ANNs not only eliminates the need of

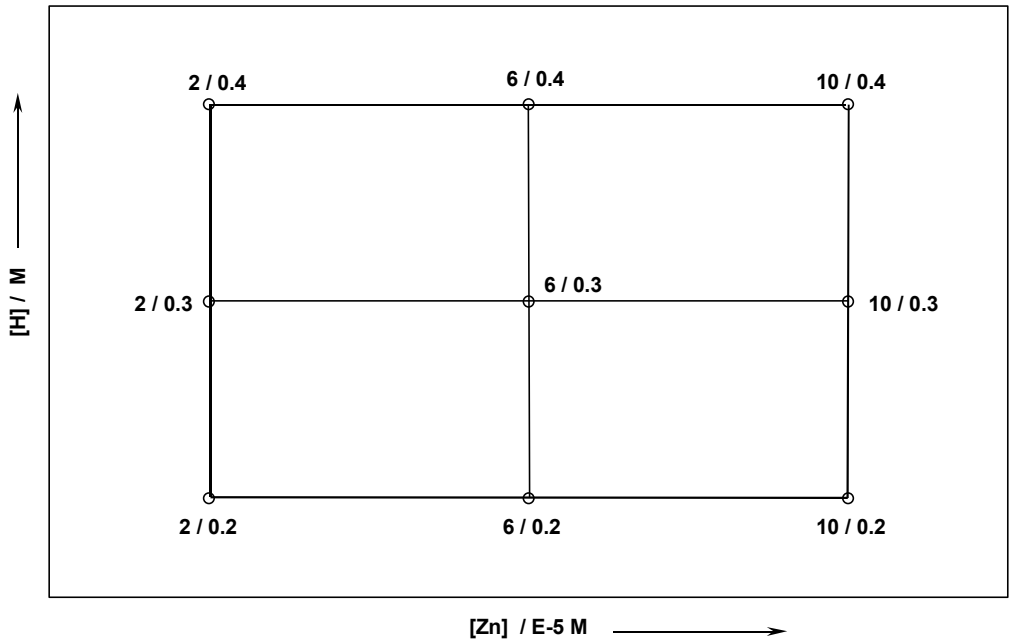

Figure 1 Experimental factorial design 3^2 (training points are seen as circles) of the calibration set for the simultaneous determination of zinc^{II} and sample acidity. For every point of the matrix, the first and the second value stands for the concentration of zinc^{II} and the acid, respectively.

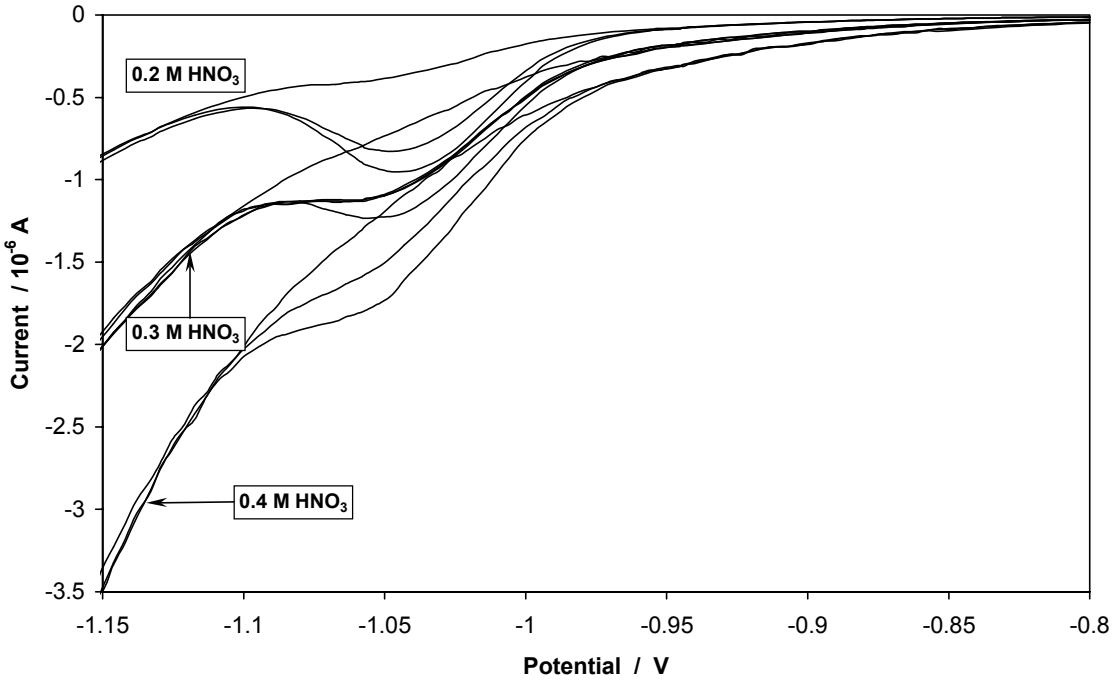

Figure 2 DP polarograms for the calibration set used for the determination of zinc^{II} and acidity of a sample. Significant reduction of hydrogen ions is observed at most negative potentials. The contribution of the zinc ions reduction to the overall current is seen in the potential range between –1 and –1.1 V.

Table 1 Results from ANNs for the simultaneous determination of Zn^{II} content and acidity of the test samples. ANNs was trained with the set of points seen in Figure 1. Δ and stdev stand for the absolute error and standard deviation, respectively.

$[Zn^{2+}]$ (x 10^{-5} M)				$[HNO_3]$ (M)			
Added	Found	Δ	% error	added	found	Δ	% error
6	6	0	0	0.4	0.399	0.001	0.25
4	4.1	0.1	2.5	0.25	0.253	0.003	1.20
7	7.1	0.1	1.43	0.25	0.255	0.005	2.00
6	6.4	0.4	6.67	0.375	0.382	0.007	1.87
8	8.5	0.5	6.25	0.375	0.380	0.005	1.33
6	5.9	0.1	1.67	0.375	0.385	0.010	2.66
3	3.2	0.2	6.67	0.375	0.384	0.009	2.40
7	7.2	0.2	2.86	0.25	0.257	0.007	2.80
		Average error:	3.51			Average error:	1.81
		Stdev:	2.64			Stdev:	0.86

the background current subtraction, but also allows to estimate the acidity of the sample studied with reasonable accuracy (with an error of about 2 %). One should note that the trained ANNs generate the output (here, the concentration of zinc and hydrogen ions) immediately. This, as well as the results discussed above, indicates the possibility of an on-line monitoring of a composition of acidic solutions. It is reasonable to assume that ANNs could also be used for the simultaneous determination of acidity and significantly lower zinc (or other metal ion) concentration by use of stripping voltammetry employed either in anodic or cathodic mode. It is well known that accurate measurement of p[H], or an acid content, by glass electrodes, when work is performed in the low p[H] region, is rather difficult task. Note that ANNs predicted the acid concentration to the third decimal place of the molar concentration (Table 1). This suggests an indirect use of ANNs to monitor p[H] of highly acidic solutions (e.g. in plating industry) from the polarographic measurement; a measurement that is p[H]-dependant, such as that discussed in this work.

3.2. Determination of Cr(III) - Zn(II) mixtures in the region of hydrogen evolution

3.2.1. Analysis by soft model (ANNs)

Several experimental designs were used to construct the calibration matrix for the resolution of chromium^{III} and zinc^{II} in 1 M perchloric acid, namely a central point composite design and two factorial designs (three level 3^2 and five level 5^2). The central training point was replicated four times in every design. Better results were obtained for factorial designs (3^2 and 5^2) and they were used for the final analysis of the test solutions.

Figure 3 shows the composition of the calibration matrix and concentrations of both metal ions for every training point (square) in the experimental design with a set of selected test points (circles) that are discussed below. For the matrix composed of 5^2 points the highest Cr : Zn concentration ratio was 50. The DP polarograms recorded for the calibration solutions are shown in Figure 4.

One can easily distinguish five subsets of curves in Figure 4 that are grouped around the particular concentration of chromium; this is not surprising as the samples contained a significant excess of chromium. The increase in the reduction current is almost identical within a subset of curves. The decrease in the reduction current (prior the reduction current attributed to the hydrogen evolution) for all curves recorded depends on the content of zinc in a sample. However, from the shape of polarograms one is unable to predict the presence of the two metal ions in a solution; the contributions from each metal ion are indistinguishable. It means that it would be impossible to predict the presence of the two metal ions in a solution just from the inspection of recorded polarograms. It is also seen that the DPP process(es) is/are highly irreversible. It was interesting to see whether the use of ANNs would allow quantifying these two metal ions with reasonable accuracy at all and, in particular, for samples that contained the concentrations of zinc and chromium not included in the training set. It was established that the best agreement between expected and computed values could be obtained from the ANNs structure containing 9 hidden neurones. Also with 13 hidden neurones similar results were obtained (the training process took about 3 hours using learning rate from 0.001 to 0.01).

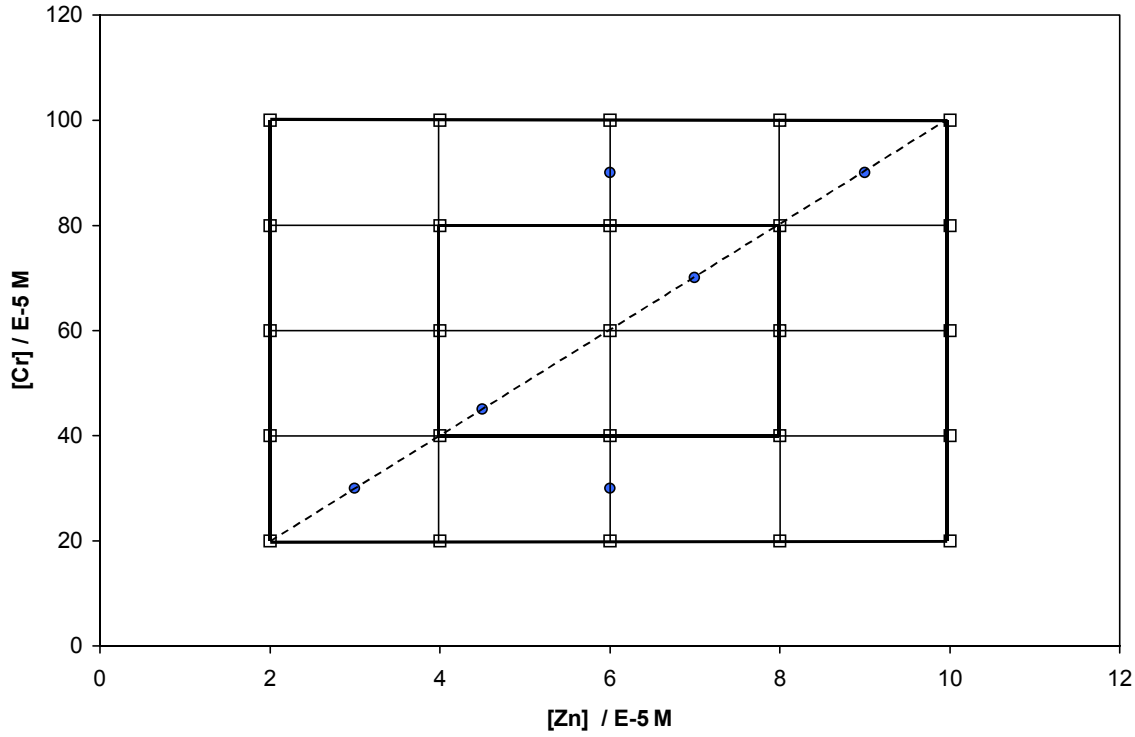

Figure 3 Experimental factorial designs 5^2 and 3^2 (training points are seen as (□)) of the calibration sets used for the simultaneous determination of zinc^{II} and chromium^{III} in 1 M perchloric acid. Selected test points are seen as (●).

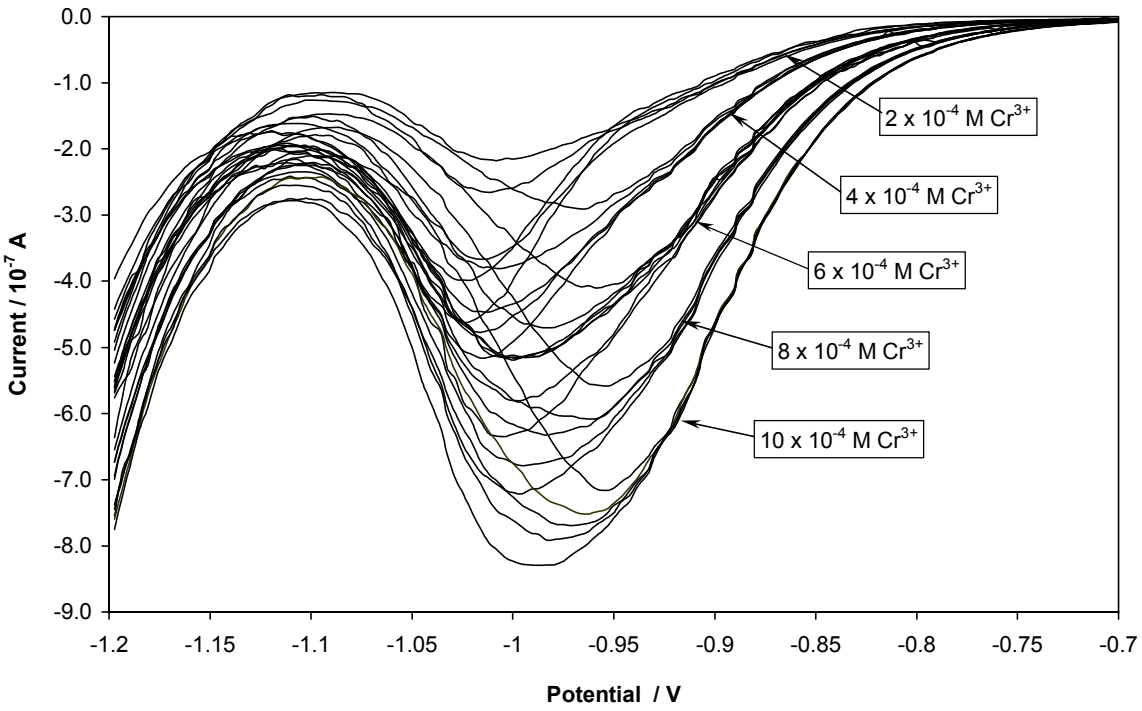

Figure 4 DP polarograms for the calibration set used for the simultaneous determination of zinc^{II} and chromium^{III} in 1 M perchloric acid; factorial design 5^2.

Table 2 shows the results for predicted and actual concentrations of the ten-point test set. It is seen that both metal ions could be quantified with similar and reasonable accuracy. When the complexity of the electrochemical process and the shape of the electrochemical signal are taken into account then the results obtained can be regarded as highly satisfactory.

The solutions from the central part of the five level factorial design (seen as a thick frame in Fig. 3, including the central point) were used to construct the three level factorial design. The highest Cr : Zn concentration ratio was in this case 20. The training of ANNs, at the same conditions as above, gave good results already for 5 hidden neurones. Accuracy in the computed concentrations was better in this case (Table 3). This clearly indicates that one can use an appropriate ED that is most suitable for particular application, depending on the expected or required accuracy in the evaluated values.

Table 2 Results from ANNs of the simultaneous determination of Zn^{II} and Cr^{III} in 1 M $HClO_4$ from the calibration matrix 5^2 seen in Figure 3. Δ and stdev stand for the absolute error and standard deviation, respectively.

$[Zn^{2+}]$ (x 10^{-5} M)				$[Cr^{3+}]$ (x 10^{-5} M)			
Added	found	Δ	% error	added	found	Δ	% error
3	2.8	0.2	6.7	30	29.6	0.4	1.3
6	5.9	0.1	1.7	30	28.0	2.0	6.7
4.5	4.3	0.2	4.2	45	43.5	1.5	3.3
8	8.4	0.4	5.0	50	46.8	3.2	6.4
3	2.8	0.2	6.7	60	58.3	1.7	2.8
9	9.2	0.2	2.2	60	61.8	1.8	3.0
5	4.6	0.4	8.0	70	73.2	3.2	4.6
7	7.3	0.3	4.3	70	74.0	4.0	5.7
6	6.2	0.2	3.3	90	92.6	2.6	2.9
9	9.3	0.3	4.4	90	95.0	5.0	5.6
		Average error:	4.7			Average error:	4.2
		Stdev:	1.8			Stdev:	1.5

From the analysis of data seen in Tables 2-3 it appears that the errors are randomly distributed; there is no apparent relationship between the error and either the chromium or zinc concentration. For example (from an analysis of data in Table 2) the largest error (8 %) for zinc happened to be for a solution 5 $\times 10^{-5}$ M Zn^{2+}, whereas for samples containing 6 $\times 10^{-5}$ M Zn^{2+}, the errors in the zinc content predicted by ANNs were 1.7 and 3.3 % in the presence of 3 $\times 10^{-4}$ and 9 $\times 10^{-4}$ M Cr^{3+}, respectively. In case of chromium, the smallest error (1.3 %) was obtained for a sample with the lowest Cr^{III} content. It is known that when hard model based optimisation procedures are used then the smallest error in estimated concentration would be expected for a sample with the highest metal ion concentration when only random errors are present. The random distribution of errors for both metal ions is important as it suggest the possibility of an on-line monitoring of these two components and the concentrations evaluated by ANNs should be within few percent, regardless on the absolute content of a metal ion in a sample. This could be hardly expected from hard models.

Table 3 Results of the simultaneous determination of Zn^{II} and Cr^{III} in 1 M $HClO_4$ from the calibration matrix 3^2 seen in Figure 3. Δ and stdev stand for the absolute error and standard deviation, respectively.

$[Zn^{2+}]$ (x 10^{-5} M)				$[Cr^{3+}]$ (x 10^{-5} M)			
Added	found	Δ	% error	added	found	Δ	% error
8	8.6	0.6	7.5	50	52.3	2.3	2.4
5	5.3	0.3	6.0	70	73.1	3.1	4.3
7	7.2	0.2	2.8	70	73.8	3.8	5.4
6.5	6.4	0.1	4.5	50	50.4	0.4	0.8
4.5	4.5	0	0	45	45.0	0	0
7	7.1	0.1	1.4	50	49.2	0.8	1.6
5.5	5.5	0	0	75	71.0	4.0	5.3
5	4.8	0.2	4.0	70	66.9	3.1	4.4
7.5	8.0	0.5	6.7	75	77.6	2.6	3.5
6	6.1	0.1	1.5	60	63.1	3.1	5.2
	Average error:		3.4		Average error:		3.3
	Stdev:		2.3		Stdev:		2.2

3.2.2. Analysis by hard model

It was of great interest to see whether one could obtain similar (or better) results with a use of 'standard' hard model based optimisation procedures that are commonly employed in non-linear curve fitting operations. An evaluation of selected training and test points, used in the analysis of the samples by ANNs, is of interest now. The test points seen in Figure 3 as circles, arranged, together with appropriate training points, were arranged in two subsets of points.

The first subset of points is connected with the dashed line seen in Figure 3. These points were selected as they should, in principle, allow constructing two calibration curves (for zinc and chromium). Note that for all those points the [Cr]:[Zn] ratio is fixed and equal to 10. Each experimental polarogram was fitted[33] with two curves for the reduction of Zn and Cr plus a background current. In each case it was possible to fit experimental curves quite well. However, the fitting operation resulted in several and significantly different values of E_p, I_p and $w_{1/2}$ (all these symbols have common meaning in DPP) for each component (Cr and Zn) with very much the same goodness of fit. One must remember that in a search for a global minimum during the refinement operation, it is necessary to repeat optimisation process for the same experimental curve several times with different initial values of fitted parameters. Because several different values were obtained for the same fitted parameters for each polarogram, an attempt was made to choose refined I_p values in such a way that one could construct as good as possible calibration plots. Results obtained are seen in Figure 5 and Table 4.

Unfortunately, it was impossible to obtain the straight calibration plot for zinc when hard model based refinement procedures were used. Circles seen in Figure 5, together with the fitted solid line described by a polynomial provided on the same Figure, represent refined I_p for the training points along the dashed line seen in Figure 3. The quantitative analysis of zinc for several test points is provided in Table 4.

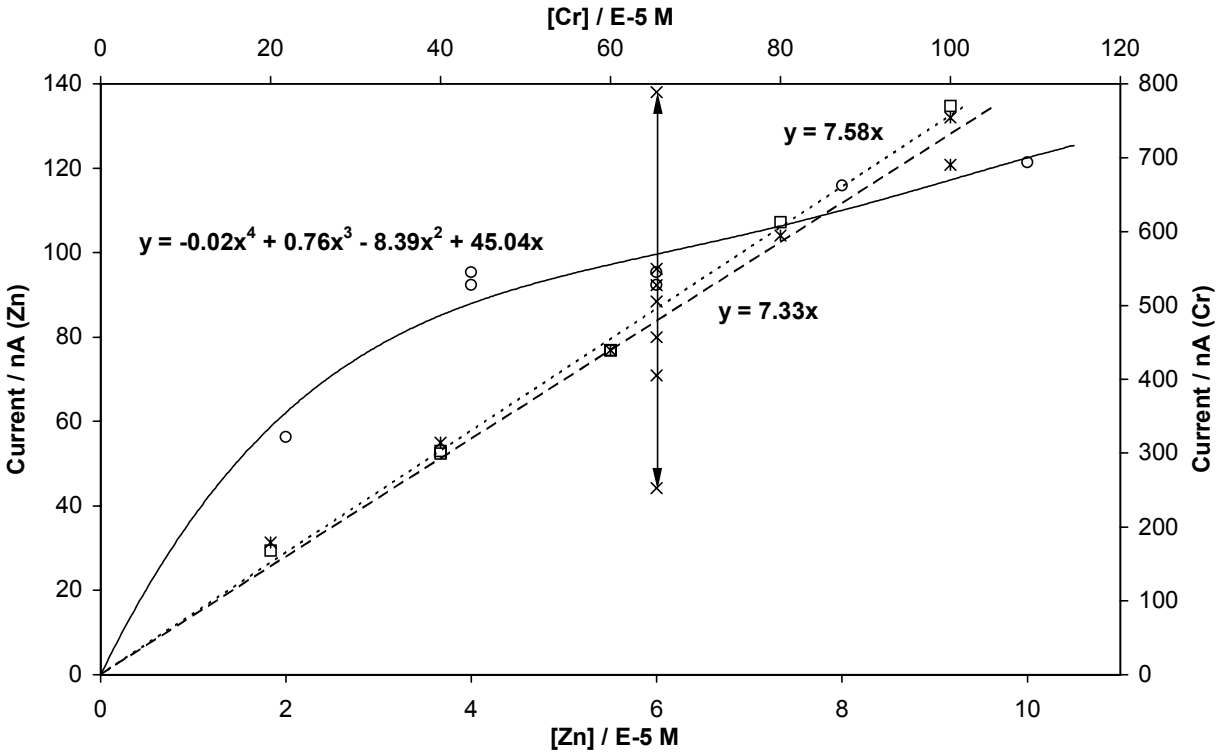

Figure 5 Variation in the peak height (obtained from the hard model fitting procedure) for zinc (○ and X) and chromium (□ and ∗). For more information see in the text.

One can see that the difference between the expected and refined I_p is unacceptably large. Note that the results seen in Table 4 are just the selected and the best optimised values, as for most training and testing points very different results were obtained from each optimisation run. In the case of the smallest content of zinc the refined I_p value was large and negative; this result suggests the absence of zinc in the sample. However, for the same test point the expected and found by ANNs values were 3×10^{-5} and 2.8×10^{-5} M Zn^{2+}, respectively. Also for the test point with higher zinc content of 7×10^{-5} M, results obtained from the hard model were very bad (expected and refined I_p were 104.5 and 402.8 nA, respectively). For the same sample ANNs made an error in the estimates for zinc and chromium of 4.3 and 5.7 %, respectively.

Table 4 Quantitative analysis of Zn^{II} and Cr^{III} contents for the selected training and test points seen in Figure 3 by a standard hard model based optimisation procedures. Values in the first column indicate concentrations (10^{-5} M) of Zn^{II} and Cr^{III}. For more details, see the text.

	Zinc			Chromium		
(a) - points from the training set along the dashed line in Figure 3						
Training point	I_p / nA	E_p / V	$w_{1/2}$ / V	I_p / nA	E_p / V	$w_{1/2}$ / V
2 / 20	56.3	-1.015	0.067	168.3	-0.978	0.180
4 / 40	95.3	-1.018	0.070	299.6	-0.983	0.175
4 / 40	92.3	-1.018	0.068	303.2	-0.984	0.174
6 / 60	92.3	-1.011	0.071	439.5	-0.976	0.169
6 / 60	95.3	-1.011	0.072	439.5	-0.976	0.169
8 / 80	115.9	-1.013	0.063	612.6	-0.971	0.166
10 / 100	121.3	-1.015	0.059	770.2	-0.970	0.166
(b) - points from the training set along vertical middle line in Figure 3						
6 / 20	88.5	-1.014	0.066	178.9	-0.985	0.188
6 / 40	138	-1.017	0.073	314.4	-0.984	0.177
6 / 60	92.3	-1.011	0.071	439.5	-0.976	0.169
6 / 80	80.0	-1.014	0.058	594.9	-0.968	0.165
6 / 100	96.2	-0.998	0.109	690.3	-0.964	0.168
6 / 100	44.2	-1.018	0.040	754.2	-0.968	0.165

(c) – selected test points

	I_p / nA		I_p / nA	
Tests points	Expected	Refined	Expected	Refined
3 / 30	78.0	Negative value	227.5	394.3
4.5 / 45	91.6	90.0	341.2	506.0
7 / 70	104.5	402.8	530.8	441.6
9 / 90	116.0	147.5	682.4	704.3

The difficulty in obtaining reasonable estimates from the hard model might be understood better when curves in Figure 6A are analysed. Curve 1 and 2 represent the samples with 3×10^{-5} plus 3×10^{-4} M, and 6×10^{-5} plus 9×10^{-4} M, of Zn^{II} and

Cr^{III}, respectively. The overall fit for most of the curves was good and similar to that observed in Figure 6. Points and solid lines represent the experimental and fitted overall polarographic current, respectively. It is seen that the contribution to the overall current comes mainly from the irreversible (see the peak width $w_{1/2}$ for chromium in Table 4) reduction of chromium. The contribution of zinc to the overall reduction current was rather small. In case of hard model based refinement procedures it was difficult to evaluate the contributions from both metal ions and the background current. Just as an example, the contributions to the overall current (curve 1) coming from each component (reduction of chromium, zinc and the background current) are seen as dotted lines in Figure 6A. In case of curve 2, one cannot visually estimate a contribution from the reduction of zinc at all. This has not been a problem when ANNs was used to evaluate the concentrations of both metal ions even though the shape of the background current varied between experimental curves. The large uncertainty in the refined values by the hard model can be appreciated from the straight vertical line seen in Figure 5. This line indicates the spread in the refined values in I_p (marked with X) for the same zinc concentration of 6 $\times 10^{-5}$ M, but coming from different samples with increasing concentration in chromium. These samples are represented by squares and circles linked with a solid vertical line in the middle of the experimental design seen in Figure 3. It was possible to obtain a reasonable straight calibration plot from the selected refined values of I_p for Cr^{III} (see the dotted line with squares in Figure 5). Squares represent the estimated current from training points placed along dashed line in Figure 3. From the analysis of the second subset of training points seen in Figure 3 at the zinc concentration of 6×10^{-5} M another calibration plot was obtained for Cr^{III} (dashed line in Figure 5). Calibration plots seen in Figure 5 were obtained from the hard model based refinement operation and only 'the best' points were selected. Often several and very different refined values were obtained from the analysis of a single polarogram. To indicate this, two values of the estimated I_p for chromium are seen as asterisks in Figure 5 for the chromium concentration of 1×10^{-3} M. In general, the estimates in the chromium content obtained from the hard model were better for Cr^{III} (but not satisfactory) than those obtained for zinc.

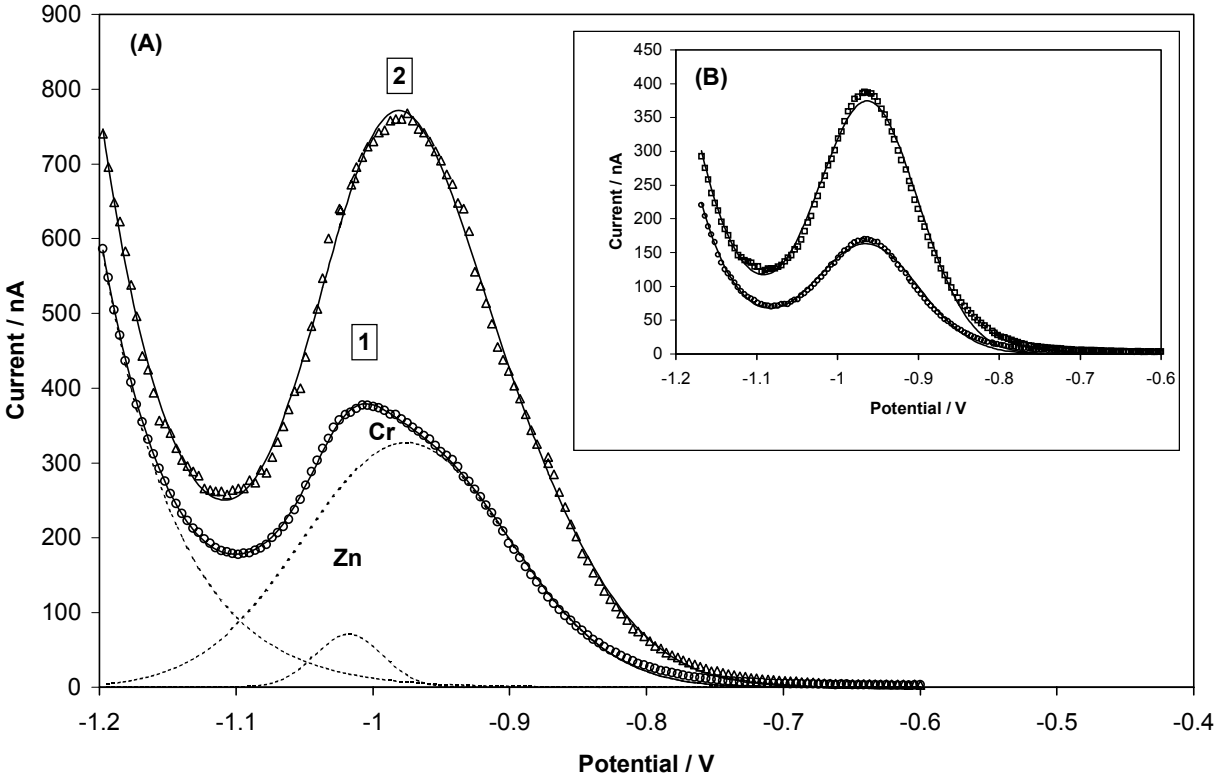

Figure 6 Examples of experimental polarograms (points) for: (A) a mixture of zinc and chromium; (B) chromium only. Solid curves - calculated polarograms with parameters obtained from the hard model. Dotted lines are components of the overall polarographic current for curve 1.

One can see that the shape of polarograms for the mixtures of zinc and chromium (Figure 6A) and for chromium only (Figure 6B) is very much the same, particularly for a higher chromium content. Here again, ANNs had no problem to estimate both components with acceptable accuracy. Opposite is true in case of the hard model. When refined values were taken (without an attempt of constructing a straight line) then results obtained for the test points of chromium were unacceptable at all - see Table 4.

From the above, it is clear that the hard model based refinement operations cannot be employed when an accurate estimate of chromium and zinc contents in an acidic medium is of interest. It seems obvious that the hard model would not be suitable for an on-line monitoring of these two elements either. On the other hand, ANNs shows a promise in conventional and in potential on-line applications when a direct analysis of samples is difficult. As a matter of fact, ANNs can also be employed in a straightforward analysis of samples.

4. Conclusions

The results obtained in this work have demonstrated that using ANNs as a soft calibration method the resolution and quantitative analysis of highly overlapped, irreversible and asymmetric electrochemical signals that also might be disturbed by a hydrogen evolution, is possible. In this respect, ANNs proved to be much more powerful, reliable and more convenient tool than the hard model based refinement procedures that proved to be useless in the cases discussed in this work. The computed by ANNs results, if required, can be improved by the use of appropriate experimental design when higher accuracy is expected. The method described has a general application, not only in electrochemistry, and provides new possibilities for an analysis of highly acidic samples, or more generally, highly disturbed by the background current and/or electron transfer electrochemical signals without a need of intervention in a sample treatment. It is important to note that the trained ANNs structure generates results of a sample immediately after the reading of a data file. This feature suggests a possibility of an 'on-line' control of, for example, plating solutions or waste control of industrial effluents.

Acknowledgements

The authors (EC and IC) thank the University of the Witwatersrand, the National Research Foundation and Masaryk University for generous financial support for this work and the Department of Analytical Chemistry of the Masaryk University for arrangements made during the sabbatical leave.

References

1 A.J. Bard and L.R. Faulkner, in *Electrochemical Methods: Fundamentals and Applications*, J. Wiley & Sons, New York, 1980.

2 A.M. Bond, in *Modern Polarographic Methods in Analytical Chemistry*, Marcel Dekker, New York, 1980.

3 P. O'Neill, in *Environmental Chemistry*, Chapman & Hall, UK, 1993.

4 *Chemical speciation in the Environment*, *Eds*.: E.M. Ure and G.M. Davidson, Blackie Academic & Professional, London, 1997.

5 D.E. Rumelhart, and J.L. McClelland, in *Parallel Distributed Processing: Explorations in the Microstructure of Cognition*, The MIT Press, Cambridge, MA, 1986.

6 J.L. McClelland, and D.E. Rumelhart, in *Explorations in Parallel Distributed Processing*, The MIT Press, Cambridge, MA, 1988.
7 L.R. Harvey, in *Neural Network Principles*, Prentice Hall, London 1994.
8 D.L. Massart, B.G.M. Vandeginste, S.M. Deming, Y. Michotte, and L. Kaufman, in *Chemometrics: A Textbook*, Elsevier, Amsterdam, 1988.
9 P. J. Gemperline, J.R. Long, and V.G. Gregoriou, *Anal. Chem*., 1991, **63**, 2313.
10 M. Bos, A. Bos, and E. van der Linden, *Analyst*, 1993, **118**, 323.
11 T. B. Blank, and S.D. Brown, *Anal. Chim. Acta*, 1993, **277**, 273.
12 B. Walczak, and W. Wegscheider, *Anal. Chim. Acta*, 1993, **283**, 508.
13 R. Goodacre, and D.B. Kell, *Anal. Chim. Acta*, 1993, **279** 17.
14 R. Goodacre, M.J. Neal, and D.B. Kell, *Anal. Chem*., 1994, **66**, 1070.
15 J. Zupan, M. Novic, X.Z. Li, and J. Gasteiger, *Anal. Chim. Acta*, 1994, **292**, 219.
16 J. Zupan, and J. Gasteiger, *Anal. Chim. Acta*, 1991, **248**, 1.
17 J. Zupan, and J. Gasteiger, in *Neural Networks for Chemists: An Introduction*, VCH, Weinheim, 1993.
18 J. Gasteiger, and J. Zupan, *J. Angew. Chem*., 1993, **32**, 503.
19 H. Miao, M. Yu, and S. Hu, *J. Chromatogr. A*, 1996, **749**, 5.
20 E. Marengo, M.C. Gennaro, and S.Angelino, *J. Chromatogr. A*, 1998, **799**, 47.
21 H. J. Metting, and P.M.J. Coenegracht, *J. Chromatogr. A*, 1996, **728**, 47.
22 J. Havel, E.M. Peña Mendez, A. Rojas-Hernández, J.-P. Doucet, and A. Panaye, *J. Chromatogr. A*, 1998, **793**, 317.
23 J. Havel, H. Breadmore, M. Macka, and P.R. Haddad, *J. Chromatogr. A*, in print.
24 T.D. Booth, K. Azzaoui, and I.W. Wainer, *Anal. Chem*., 1997, **69**, 3879.
25 V. Dohnal, M. Farkova, and J. Havel, *Chirality*, in press.
26 J. Havel, J. Madden, and P.R. Haddad, *Chromatographia*, in press.
27 H. Chan, A. Butler, D.M. Falck, and M.S. Freund, *Anal. Chem*., 1997, **69**, 2373.
28 J. Alpizar, A. Cladera, V. Cerda, E. Lastres, L. Garcia, and M. Catasus, *Anal. Chim. Acta*, 1997, **340**, 149.
29 A. Cladera, J. Alpizar, J.M. Estela, V. Cerda, M. Catasus and L. Garcia, *Anal. Chim. Acta*, 1997, **350**, 163.
30 Yu.G. Vlasov, A.V. Legin, A.M. Rudnitskaya, A. D'amico and C. Di Natale, *J. Anal. Chem*., 1997, **52**, 1087.
31 S.N. Deming, and S.L. Morgan, in *Experimental Design: A Chemometric Approach*, Elsevier, Amsterdam, 1989.

32 D.L. Massart, B.G.M. Vandeginste, L.M.C. Buydens, S. de Jong, P.J. Levi, and J. Smeyers-Verbeke, in *Handbook of Chemometrics and Qualimetrics: Part A*, Elsevier, 1997.

33 I. Cukrowski, *J. Electroanal Chem.*, 1999, **460**, 197.